

GPS Estimates of Postglacial Uplift in Fennoscandia

Klaus Kaniuth and Sandra Vetter

Summary

Due to ongoing postglacial rebound Fennoscandia is subject to land uplift. In order to determine the present-day uplift rates, a network of permanent GPS stations is analysed. Three years of continuous GPS measurements between October 2000 and September 2003 are processed. The uplift rates estimated in a geocentric reference frame reach as much as 9 mm/yr in the central part of the uplift area. Besides these linear velocities various other parameters are estimated in a common adjustment. These include mean ellipsoidal station heights, referring to epoch 2002.0 and a local reference pressure, and height discontinuities due to antenna configuration changes. In addition, site dependent atmospheric pressure loading coefficients, annual sinusoidal signals as well as irregular and short-period local height biases are estimated. It seems that the latter phenomenon can be attributed to snow accumulation on the GPS antenna.

Zusammenfassung

Als Folge anhaltender postglazialer isostatischer Ausgleichsbewegung kommt es in Fennoskandien zu Landhebungen. Um die Größe der derzeitigen Höhenbewegungen zu bestimmen, wird ein Netz von permanenten GPS-Stationen analysiert. Dazu werden drei Jahre kontinuierlicher GPS-Messungen von Oktober 2000 bis September 2003 ausgewertet. Die in einem geozentrischen Referenzsystem bestimmten Höhenbewegungen erreichen bis zu 9 mm/a im Zentrum Fennoskandiens. Neben diesen linearen vertikalen Geschwindigkeiten wird eine Reihe weiterer Parameter in einer gemeinsamen Ausgleichung geschätzt. Dazu gehören die mittleren ellipsoidischen Höhen aller Stationen, die sich auf die Epoche 2002.0 und auf einen lokalen Referenzluftdruck beziehen, und durch Änderung von Antennenkonfigurationen bedingte Sprünge in den geschätzten Höhen. Zusätzlich werden stationsabhängige atmosphärische Druckauflastkoeffizienten, Signale mit Jahresperiode sowie unregelmäßige und kurzzeitige lokale systematische Höhenfehler geschätzt. Es scheint, dass der letztgenannte Effekt durch Akkumulation von Schnee auf GPS-Antennen hervorgerufen wird.

1 Introduction

Due to the ongoing postglacial isostatic adjustment Fennoscandia is subject to land uplift with reported rates of as much as 10 mm/yr in the centre. Prior to the advent of space geodetic techniques the phenomenon has been studied by analysing ancient time series of sea level variations, modern tide gauge records or the results of repeated precise levellings. From 1990 on permanent Global Positioning System (GPS) stations were installed

in Norway, Sweden, Finland and Denmark. In 1993, the project BIFROST (Baseline Inferences for Fennoscandian Rebound Observations, Sea level and Tectonics) was established comprising stations of the Swedish and Finnish permanent GPS networks. An extensive analysis of the BIFROST observations was performed by Johansson et al. (2002). This study included data collected between August 1993 and May 2000 and had to cope with a large number of instrumental changes during the early years. It includes a thorough discussion of error sources and yields formal errors of 0.2 mm/yr for the vertical velocities. Based on a time series of daily BIFROST position estimates covering the same period, Scherneck et al. (2003) have recently investigated the robustness of velocity estimates by studying the impact of loading effects due to ocean, atmosphere and hydrology on the estimated velocities. Mäkinen et al. (2003) determined vertical velocities of the Finnish permanent GPS stations and compared them with results from repeated precise levelling. The processed GPS data cover the period from October 1996 to October 2001, and the analysis is based on weekly solutions. Accuracies of 0.4 mm/yr are quoted for the uplift rates.

As the cited studies do not include the most recent observations, we have processed – in this analysis – a data set covering the three years period from October 2000 to September 2003. Blewitt and Lavallée (2002a, 2002b) proved theoretically and with real observations that a data span of three years is sufficiently long as to avoid biases in the estimated velocities due to annual signals, which are often present in GPS coordinate time series, particularly in the vertical component. Unfortunately, only parts of the observations acquired by the national permanent GPS networks are available to the public. This applies to all stations included in the European permanent GPS network or the global network of the International GPS Service (IGS) respectively. Thus, the analysed network comprises only these stations, and consequently the density is more sparse than in the previous studies. In the sequel the network design, the data processing characteristics and the adjustment strategy are described, and finally the obtained results are discussed.

2 GPS Network

The GPS network selected for this study is displayed in Fig. 1. The four-character identifications are those used by the GPS services. Besides all stations available in Fennoscandia itself we have for various reasons included a number of additional sites. RIGA and SVTL might both

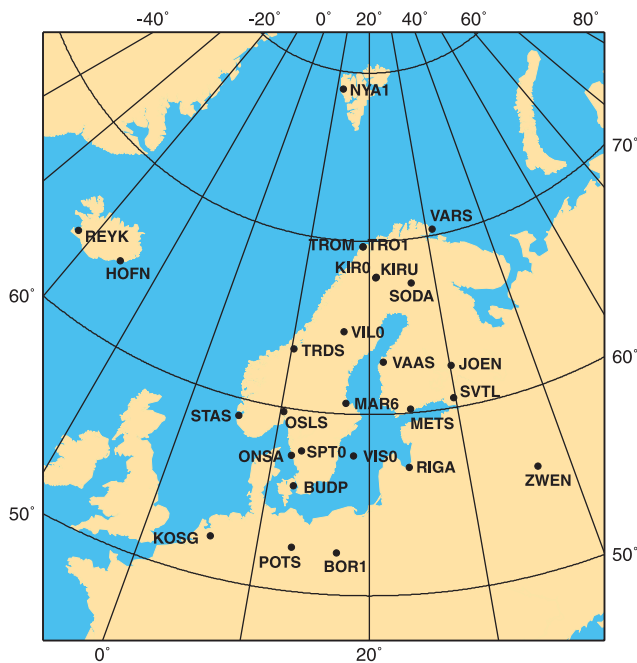


Fig. 1: Analysed network of permanent GPS stations

belong to the boundary zone of the uplift area and might therefore also experience vertical crustal motion. BOR1, KOSG, NYA1, POTS, REYK and ZWEN surrounding the study area were selected for serving as reference stations in the realisation of the reference frame, because they are the closest sites of high performance in the International Terrestrial Reference Frame 2000, ITRF2000 (Altamimi et al. 2002). Tab. 1 lists the ellipsoidal heights for these six stations at epoch 2002.0 and the vertical velocities from ITRF 2000, both with their standard deviations. HOFN on Iceland is included as an intermediate point between REYK and the sites at the Norwegian coast, in order to improve ambiguity fixing on the long baselines. The network comprises the two co-located stations TROM and TRO1, whose antennae operate at the same site in a distance of 51 m. Thus, we can assume that both experience exactly the same uplift rate, and therefore the difference between the obtained results could be an indication of the reliability of the estimated velocities. About the same applies to KIRØ and KIRU located at a distance of 4.4 km from each other. Tab. 2 lists the receiver and antenna types operated at the involved stations. The table documents also whether or not the antenna is equipped with a radome, because these protective covers affect the

Tab. 1: Ellipsoidal heights at epoch 2002.0 and vertical velocities of reference stations from ITRF 2000

Station	Height [m]	Velocity [mm/yr]
BOR1	124.366 ± 0.002	-1.1 ± 0.6
KOSG	96.856 ± 0.002	0.7 ± 0.5
NYA1	84.213 ± 0.004	6.4 ± 0.6
POTS	144.418 ± 0.002	-1.3 ± 0.4
REYK	93.047 ± 0.002	-1.2 ± 0.7
ZWEN	204.988 ± 0.002	-2.9 ± 0.7

Tab. 2: GPS stations included in the analysis: antenna type, radome and height of antenna reference point above marker

Station	Type	Radome	Height [m]
BOR1	AOAD/M_T		0.0624
BUDP	ASH701941.B	UNAV	0.0000
HOFN	TRM22020.00+GP	DOME	0.0550
	TRM29659.00		0.0510 *
JOEN	ASH700936 A_M	SNOW	0.0000
KIRØ	AOAD/M_T	OSOD	0.0710
KIRU	ASH701945 C_M		0.0620
	ASH701945 C_M	SNOW	0.0620 *
KOSG	AOAD/M_B	DUTD	0.1050
MAR6	AOAD/M_T	OSOD	0.0710
METS	AOAD/M_B		0.0000
NYA1	ASH701073.1	SNOW	0.0000
ONSA	AOAD/M_B	OSOD	0.9950
OSLS	TRM29659.00		5.4960
POTS	AOAD/M_T		0.0460
REYK	AOAD/M_T		0.0680
	AOAD/M_T		0.0555 *
RIGA	ASH700936 D_M		0.0850
SODA	AOAD/M_T	DUTD	0.0000
SPTØ	AOAD/M_T	OSOD	0.0710
STAS	TRM29659.00	SCIS	5.5590
SVTL	TRM14532.00		0.0085
TRDS	TRM29659.00	SCIS	5.5460
TRO1	ASH701073.1	SCIS	0.0000
TROM	AOAD/M_B		2.4750
VAAS	ASH700936 A_M	SNOW	0.0000
VARS	TRM29659.00	SCIS	5.5120
VILØ	AOAD/M_T	OSOD	0.0710
VISØ	AOAD/M_T	OSOD	0.0710
ZWEN	AOAD/M_T		0.0460

* Configuration changes at HOFN on 2001-09-21, at KIRU on 2003-03-12, at REYK on 2003-06-13

height estimates (Kaniuth and Huber 2003a). The height of the antenna reference point above marker used throughout this analysis is also included. As can be seen, there occurred only three antenna configuration changes at HOFN, KIRU and REYK during the entire three years period. Most of the stations operated continuously with only few data losses. Unfortunately, observations from SPTØ and BUDP were only available since September 2001 and December 2002 respectively.

3 Daily Network Processing

The Bernese GPS software version 4.2 (Hugentobler et al. 2001) was used for processing each of the 1095 days of data. The main characteristic of this software system is that it applies the so-called double difference approach by processing between stations and between satellites

observation differences. This strategy requires the definition of baselines for creating between stations single difference observation files. The selection of baselines was not done automatically according to any fixed scheme, but has been optimized with respect to the daily data distribution in order to fully exploit the available observations. As already mentioned, identical uplift rates could be expected for TROM and TRO1 as well as for KIRU and KIRØ. Therefore, we also did not create the baselines TROM-TRO1 and KIRU-KIRØ in order to achieve, as far as possible, independent results, instead of taking advantage of the extremely short distances. Due to the proximity of the stations, the estimated local troposphere parameters would be highly correlated, and thus the correlations between the uplift rate estimates could also increase. With regard to the vertical position component the main features of the preprocessing and the daily network adjustments can be summarized as follows:

- Satellite orbits, satellite clock offsets and Earth orientation parameters fixed to the combined IGS solutions; orbits relating to earlier ITRF realisations were transformed to ITRF2000.
- The phase ambiguities were resolved applying the Quasi Ionosphere Free (QIF) strategy, resulting in a success rate of about 80% and depending slightly on baseline length and geographic latitude.
- The periodic site displacements due to ocean tides loading were modelled according to the FES99 model which is an extension of the hydrodynamic ocean tide model FES98 (Lefèvre et al. 2000).
- The elevation mask and the data sampling rate were set to 10° and 30 seconds respectively; the phase observations were weighted according to $\cos^2z + 0.3 \sin^2z$, with z being the zenith distance; this weight function is proposed by Huber and Kaniuth (2004).
- No automatic outlier rejection has been applied; instead, whenever necessary, the single baseline adjustment residuals were edited for identifying possibly un-repaired cycle slips.
- The total tropospheric zenith path delay was estimated unconstrained for each one hour interval from the GPS data itself in the daily network adjustment; the Niell (1996) mapping function was applied to the total delay.

Apart from the fact that satellite orbits and clock offsets as well as Earth orientation parameters were held fixed, the daily network adjustments are not constrained. The resulting position estimates of all involved stations and their fully occupied covariance matrix were introduced into a further adjustment, which is described in chapter 5.

4 Single Baseline Analyses

Although the baseline composition has been optimized with respect to the daily data availability, several

station combinations are available almost continuously throughout the entire three years period. These allow to study in details the time series of daily baseline component estimates and to identify any systematic effects, which are not yet appropriately modeled. The Fig. 2, 3 and 4 display – for three baselines – the deviations of the daily height difference estimates from the mean value over the three years. After solving for a linear trend and an annual period the station combination METS-MAR6 shows an r.m.s. scatter of only 3.9 mm for the daily height differences, and there is no indication of any remaining systematic effects. On the contrary, the baseline VILØ-VAAS exhibits a much larger postfit scatter of 6.5 mm and also several offsets lasting for about one to three weeks. In order to verify which of the two involved sites is responsible for these biases, Fig. 4 shows the daily height difference estimates relative to the mean value for the baseline VILØ-TRDS. The gap at the beginning of the time series is due to the fact that observations from TRDS were not available before early November 2000. The r.m.s. postfit scatter on this baseline is 5.2 mm. Small gaps in all three time series are due to missing data. A comparison of Fig. 3 and 4 clearly indicates that the apparent height jumps must be caused by the data from VAAS. Considering the distance between VILØ and VAAS of only 321 km these effects can hardly be attributed to pressure anomalies. As a consequence, there is a need to account for such biases, occurring at several sites, in the combined adjustment.

5 Combined Adjustment

The results of the daily network adjustments with the Bernese software as described in section 3 are sets of coordinate solutions with their associated fully occupied covariance matrices. They are introduced as correlated observations into a common adjustment of all 1095 days. The following parameter types are defined and solved in this adjustment:

- Mean ellipsoidal station heights h_0 referring to epoch 2002.0 and to a local reference pressure, because pressure variations cause displacements in vertical direction (Kaniuth and Huber 2003b);
- Pressure loading coefficients Δh_P for each site, accounting for the vertical displacements due to pressure variations;
- Linear vertical velocities Δh_V which are in this study the target parameters for the Fennoscandian sites;
- Sine and cosine amplitudes A_S and A_C of periodic annual height variations;
- Height discontinuities Δh_A due to antenna configuration changes as indicated in Tab. 1;
- Short period local height biases Δh_S identified in the analysis of either the baseline time series or the residuals of this combined adjustment.

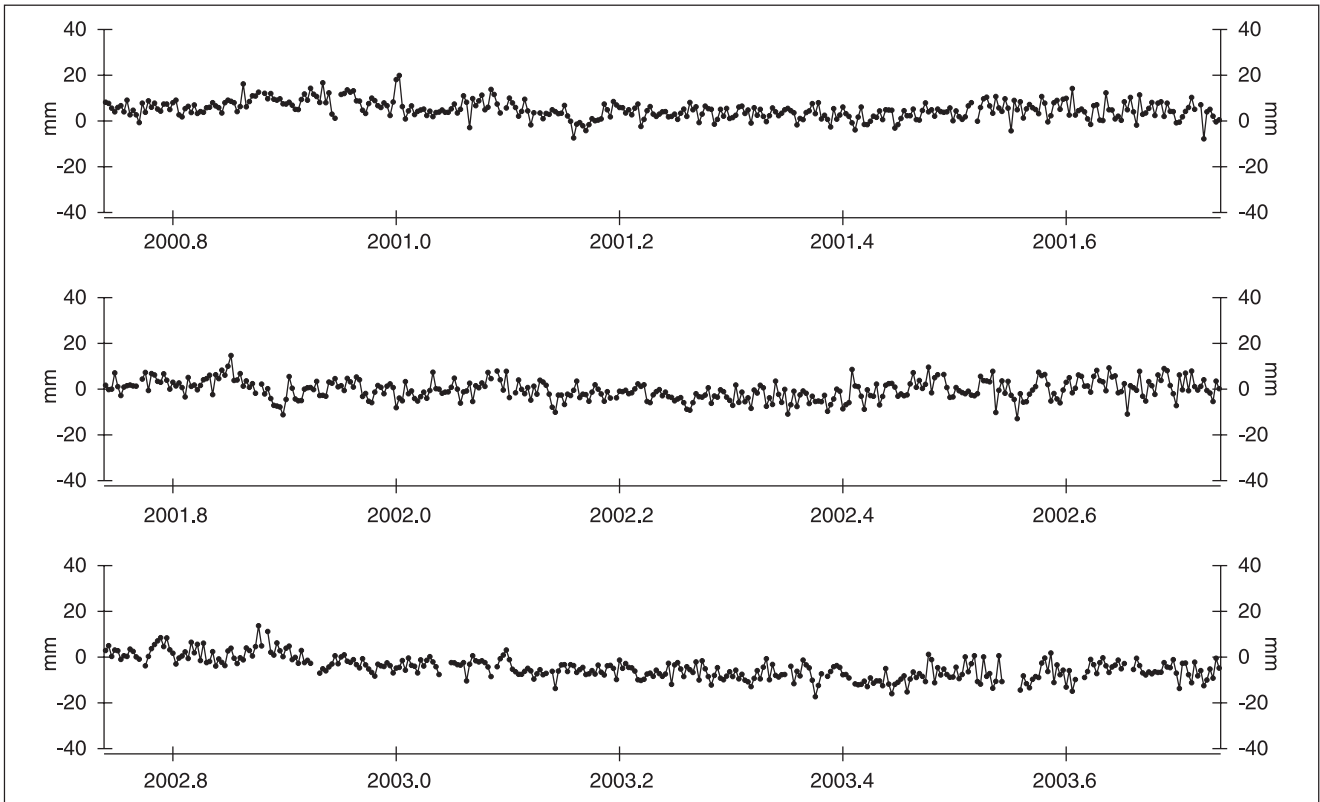


Fig. 2: Daily height differences between METS and MAR6 relative to the mean 19.1774 m during the analysed three years period

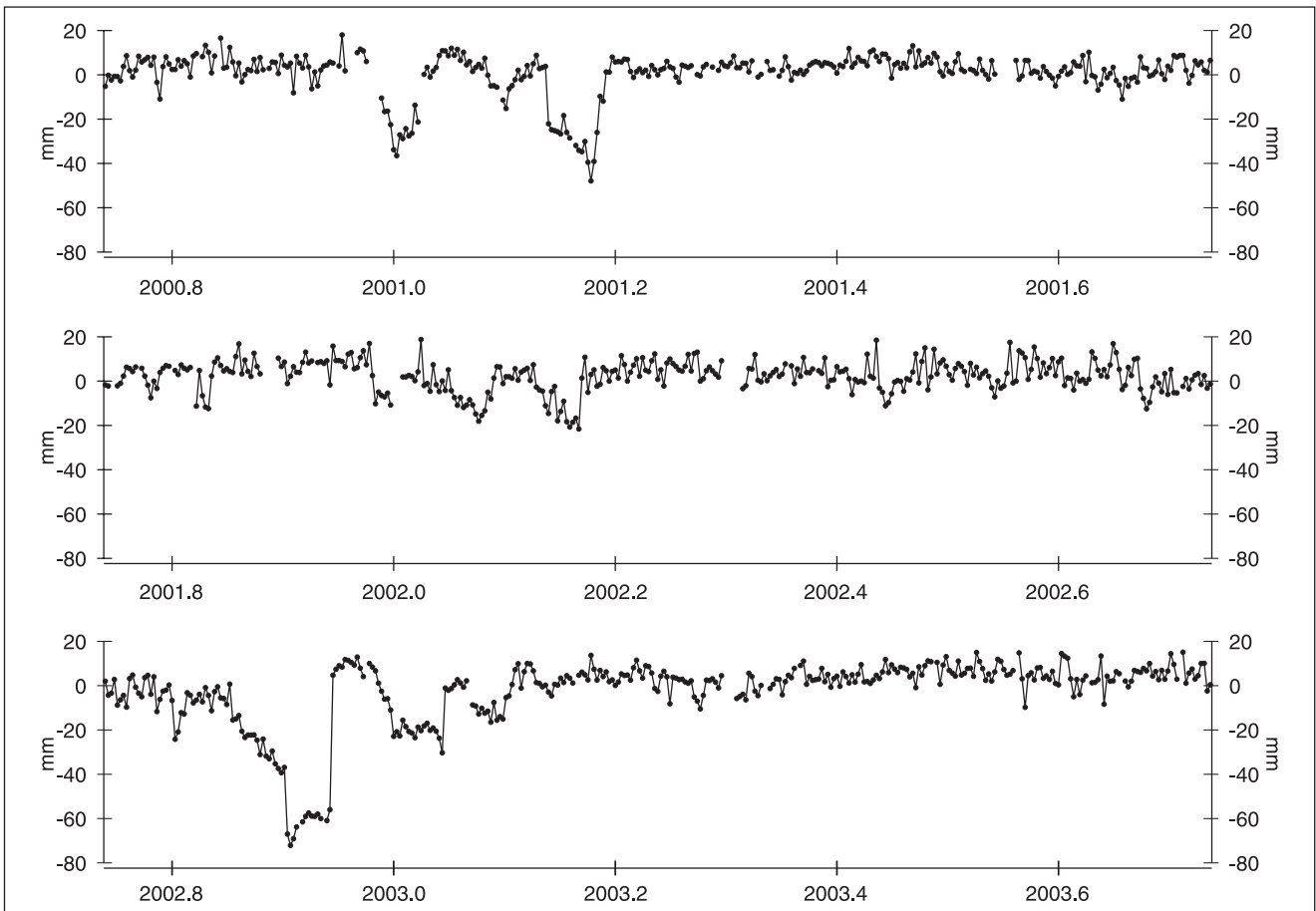


Fig. 3: Daily height differences between VILØ and VAAS relative to the mean 391.8925 m during the analysed three years period

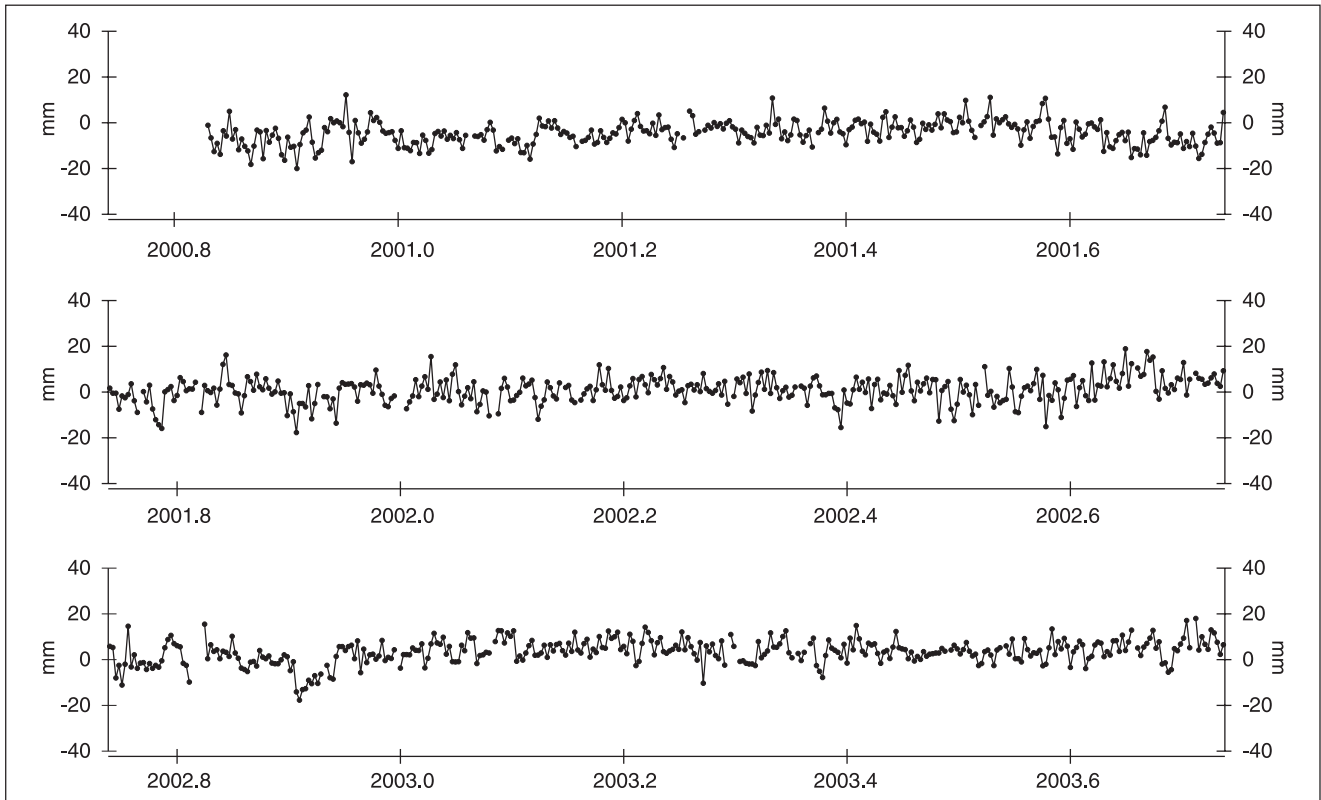


Fig. 4: Daily height differences between VILØ and TRDS relative to the mean 132.2774 m during the analysed three years period

The observation equation for an observed ellipsoidal height difference Δh^{ik} between two stations i and k then reads:

$$\begin{aligned}
 &h_0^i - h_0^k + \Delta P^i \cdot \Delta h_p^i - \Delta P^k \cdot \Delta h_p^k + \Delta T \cdot (\Delta h_v^i - \Delta h_v^k) \\
 &+ \sin(2\pi\Delta T) \cdot (A_S^i - A_S^k) + \cos(2\pi\Delta T) \cdot (A_C^i - A_C^k) \\
 &+ \Delta h_A^i - \Delta h_A^k + \Delta h_S^i - \Delta h_S^k = \Delta h^{ik} + v^{ik} \quad (1)
 \end{aligned}$$

with ΔP = Pressure anomaly [hPa],
 ΔT = Time difference to 2002.0 [years].

Note that the parameters Δh_A and Δh_S apply only to a few periods and stations.

The pressure data used in this study are daily averages for a global $2.5^\circ \times 2.5^\circ$ grid available from the National Center for Atmospheric Research (NCAR), Boulder/Colorado, USA. These grid values refer to sea level and were transformed to the ellipsoidal heights of the involved stations by using a standard formula for estimating the pressure decrease with height (Hugentobler et al. 2001) and by accounting for the geoid undulations of the EGM96 geopotential model (Lemoine et al. 1998). The local pressure at the antenna location was then derived by linear interpolation between the nearest grid points. The reference pressure for each site was defined as the mean value over the three years period.

Regarding the station heights, each daily coordinate solution experiences a small offset in radial direction due to the double differencing approach. This bias is elimi-

nated by performing a transformation from ellipsoidal heights to ellipsoidal height differences. This leads necessarily to a loss of absolute height information. Therefore, the heights and vertical velocities of the selected reference stations listed in Tab. 1 are introduced into the adjustment in order to refer the estimated uplift rates to ITRF2000. We do not simply fix the reference stations, but allow two different approaches. One is a fiducial concept applying appropriate weights to the heights and velocities of the reference stations; the other is the application of condition equations, constraining the sums of height and velocity differences between the free network and ITRF2000 to zero. This combined adjustment of all 1095 days is done with a program developed in the course of this study. A rough flow chart is given in Fig. 5.

6 Results

Some parameters were only included in the common adjustment in order to avoid impacts of unmodeled effects on the estimated uplift rates, and these are not documented in the sequel. This holds in particular for the height discontinuities due to antenna configuration changes. We neither discuss the estimated site dependent pressure loading coefficients, because this was already the subject of a recent analysis (Kaniuth and Huber 2003b). Moreover, it is planned to study this effect further by extending the network to the entire European

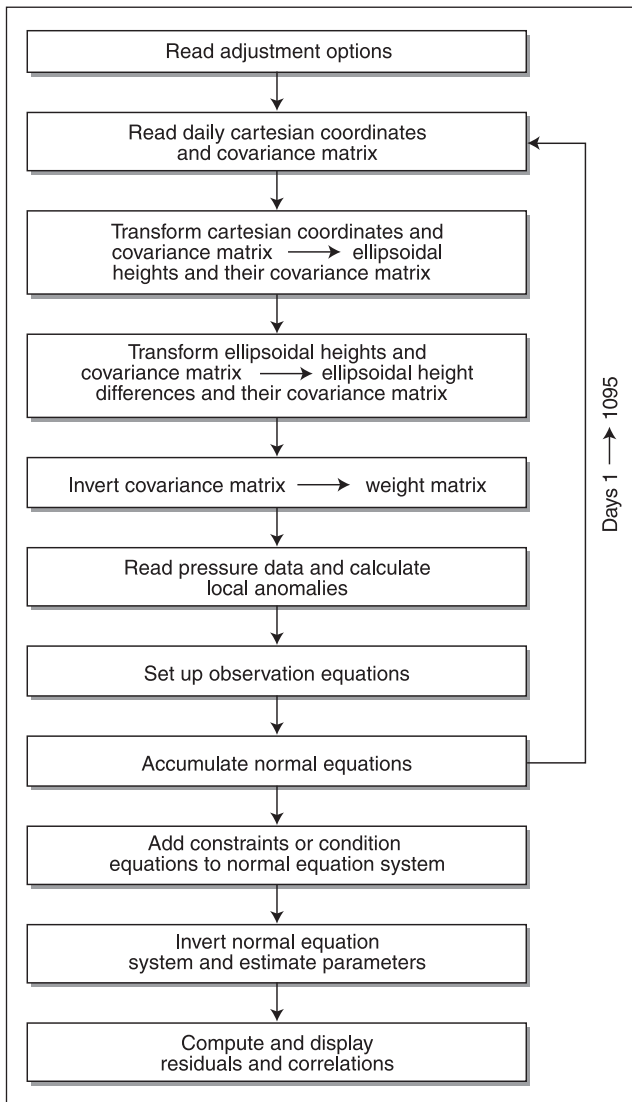


Fig. 5: Flow chart of the program developed for estimating uplift rates

continent and by including primarily all permanent GPS stations located at coastlines or on islands. However, the present results indicate that the previous analysis slightly overestimated the loading effects, because we did not solve for short period height biases at that time as we do now.

The results obtained for the identified periods of biased height estimates are given in Tab. 3 in the sequence of their occurrence. All these periods fall into winter time, and there is a concentration during the last winter 2002/2003. The standard deviations clearly prove that all estimated offsets are highly significant, although some of them represent only a time span of one to two weeks. The height biases were modeled as constants even though the examples in Fig. 3 indicate that in some cases a higher order function would be more appropriate. The largest bias at VAAS end of 2002, rapidly increasing during the first two weeks, has been modeled by two terms. Except one, all estimated offsets are positive, i. e. the station heights are apparently raised. An explanation would be that antennae or antenna radomes were

Tab. 3: Height offsets estimated for the identified biased periods

Station	Period (Year : Day)	Offset [mm]
VARS	2000 : 324 – 2000 : 340	19.5 ± 1.0
VAAS	2000 : 365 – 2001 : 010	22.4 ± 0.8
SVTL	2001 : 001 – 2001 : 007	38.9 ± 1.5
KIRU	2001 : 045 – 2001 : 086	31.6 ± 0.5
VAAS	2001 : 052 – 2001 : 070	33.1 ± 0.7
KIRU	2002 : 047 – 2002 : 075	51.7 ± 0.7
SODA	2002 : 299 – 2002 : 314	-22.5 ± 0.8
VAAS	2002 : 315 – 2002 : 330	18.5 ± 0.7
VAAS	2002 : 331 – 2002 : 345	60.7 ± 0.9
SVTL	2002 : 356 – 2002 : 008	34.9 ± 1.0
JOEN	2002 : 364 – 2003 : 017	28.0 ± 0.7
RIGA	2002 : 365 – 2003 : 008	34.8 ± 1.0
VAAS	2003 : 001 – 2003 : 017	23.1 ± 0.7
SODA	2003 : 016 – 2003 : 046	16.7 ± 0.7

covered by snow during these periods. Similar effects were already observed at a few stations of the Swedish permanent GPS network (Jaldehyg et al. 1996). Snow most likely changes the electrical properties of the antennae and leads to a positive height change of the electrical phase center, opposite in sign to the very small snow loading effect itself (see Scherneck et al. 2003). The absolute values reach several centimetres with a maximum of six in this analysis, and they can exceed even the loading displacements caused by extreme pressure lows. The small correlations between pressure loading parameters and short period height biases prove that the estimates are independent of each other.

Concerning the sine and cosine amplitudes of annual signals it should be mentioned that these could not be estimated for BUDP contributing only 281 days of data. Moreover, as the observables in the adjustment are ellipsoidal height differences the normal equation system is close to singularity when estimating absolute amplitudes for each site. Therefore, BOR1 showing the smallest annual signal has been constrained to zero. Thus, all estimates are relative to this site. On the average, the amplitudes are rather small with standard deviations of 0.3 mm and they exceed 3 mm at only five stations. The annual height variations for these are displayed in Fig. 6. The largest amplitude of 7.6 mm shows up at SODA, followed by ZWEN with 6.8 mm. As can be seen, the three stations HOFN, NYA1 and SODA are well in phase, and the same holds for RIGA and ZWEN. As expected, the correlations demonstrate that the estimation of amplitudes and phases of height variations with annual period does not at all affect the linear vertical velocities.

As described in section 5 the combined adjustment was performed applying two different approaches for realising the reference frame. These two strategies did not yield any significant differences in the adjustment results discussed so far. However, the two approaches lead to differences in the ellipsoidal heights at 2002.0 and the

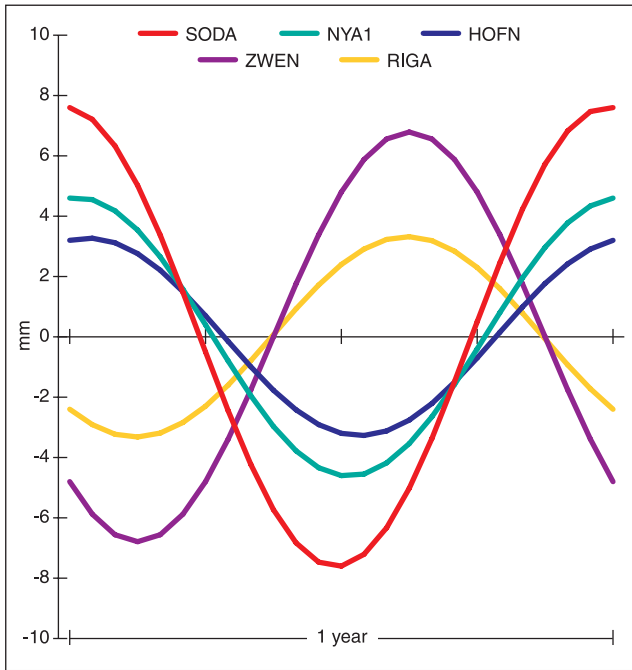


Fig. 6: Annual signals with amplitudes larger than 3 mm

vertical velocities of the reference stations of a few millimetres and a few tenth of millimetres respectively. As a consequence, the estimated uplift rates of all stations differ systematically by 0.2 mm/yr. Tab. 4 lists the results for the Fennoscandian sites from both strategies and includes also RIGA and SVTL. The velocity estimates for BUDP should be ignored in view of the large standard deviation which is due to the short time span of available observations. The systematic difference of 0.2 mm/yr clearly demonstrates the sensitivity of the vertical velocity estimates to the approach applied for fixing the kinematic reference frame. This is particularly important if the GPS network solution is based on the concept of double difference observations. As the fiducial concept may lead to small network distortions, the second approach is preferred leaving the solution internally completely unconstrained but referring it to ITRF2000 by applying two condition equations. These constrain the sum of the differences between the vertical velocities of the six reference stations from the adjustment and from ITRF2000 and also the sum of the height differences at epoch 2002.0 to zero. Fig. 7 displays the uplift rates resulting from this strategy.

Tab. 5 compares the estimated vertical velocities with those given in Johansson et al. (2002). We include two solutions from that analysis, which differ by the applied data rejection criteria and the parameterisation: one of the solutions included admittance parameters for atmospheric loading and in addition to the annual signals periodic terms with frequencies of two and three cycles per year. The results by Mäkinen et al. (2003) are not shown because there are only three stations in common and the estimated uplift rates are given only relative to METS. Instead, Tab. 5 includes the vertical velocities from ITRF2000 for those four stations whose standard devia-

Tab. 4: Uplift rates in the Fennoscandian area resulting from the two strategies applied to the stations realizing the reference frame; strategy I = weighting, strategy II = condition equation

Station	Days	Uplift Rate [mm/yr]	
		Strategy I	Strategy II
BUDP	281	3.0 ± 1.72	3.1 ± 1.68
JOEN	1055	3.7 ± 0.13	3.9 ± 0.13
KIRØ	1085	5.1 ± 0.13	5.4 ± 0.14
KIRU	1058	4.8 ± 0.15	5.0 ± 0.15
MAR6	1084	7.9 ± 0.12	8.1 ± 0.12
METS	1077	3.5 ± 0.12	3.7 ± 0.12
ONSA	1079	3.6 ± 0.12	3.8 ± 0.12
OSLS	1043	7.1 ± 0.12	7.3 ± 0.12
RIGA	1079	0.6 ± 0.14	0.7 ± 0.14
SODA	1033	7.8 ± 0.14	8.0 ± 0.15
SPTØ	733	2.2 ± 0.21	2.4 ± 0.20
STAS	1033	2.9 ± 0.12	3.1 ± 0.12
SVTL	926	0.0 ± 0.23	0.2 ± 0.20
TRDS	1036	4.5 ± 0.15	4.7 ± 0.13
TRO1	1061	0.7 ± 0.14	0.9 ± 0.15
TROM	1066	0.4 ± 0.13	0.7 ± 0.14
VAAS	1038	8.2 ± 0.16	8.4 ± 0.13
VARS	1025	-2.2 ± 0.12	-2.0 ± 0.16
VILØ	1084	9.1 ± 0.12	9.3 ± 0.12
VISØ	1078	3.2 ± 0.16	3.4 ± 0.12

tions are below one mm/yr. This holds for KIRU, METS, ONSA and TROM. The r.m.s. difference of 0.7 mm/yr between the two solutions by Johansson et al. (2002) indicates the sensitivity to modifications in the parameterisation or the data editing. The differences between those results and ours may be partly due to the reference frame realisation and the data rejection strategies. In contrast to Johansson et al. (2002) we solved explicitly

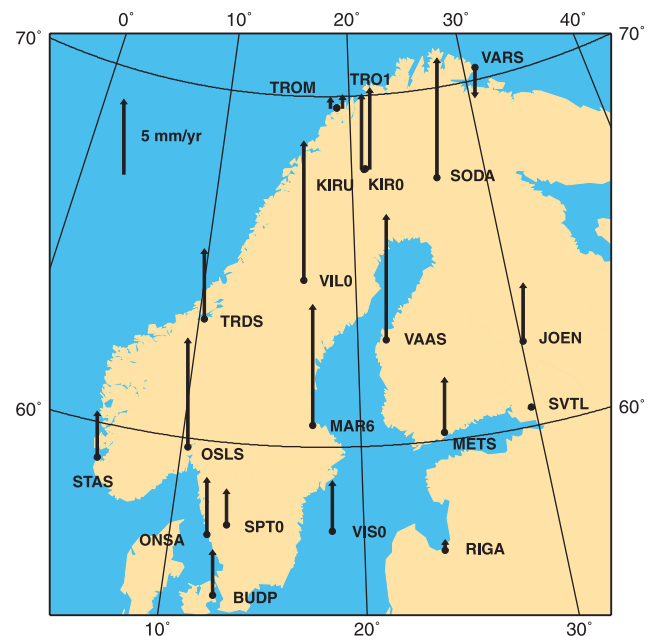


Fig. 7: Uplift rates in the Fennoscandian area

Tab. 5: Comparison of vertical velocity estimates [mm/yr]

Station	ITRF2000	Johansson et al. (2002)	This study Strategy II
JOEN		5.1	5.0
KIRU	7.2	8.5	7.0
MAR6		7.3	7.4
METS	3.5	5.4	4.6
ONSA	2.6	-0.4	-0.6
SODA		9.8	10.3
TROM	2.6	4.0	3.9
VAAS		10.7	10.1
VILØ		9.0	8.5
VISØ		3.2	2.5

for short period height biases probably caused by snow accumulation. It should also be noted that there are no observations in common. The largest discrepancies appear for ONSA and TROM. Independent Very Long Baseline Interferometry (VLBI) results for ONSA quote a vertical velocity similar to the ITRF2000 value, and in the case of TROM a display of the height time series given in Johansson et al. (2002) seems to indicate that the uplift rate is indeed close to zero since around 1999.

7 Conclusions

Uplift rates due to postglacial rebound in Fennoscandia were estimated from three years of continuous GPS observations between October 2000 and September 2003. The solution is referred to ITRF2000; however, the absolute level of the velocity field depends slightly on the approach applied for realising the reference frame. The standard deviations of the estimated vertical velocities resulting from a common adjustment of 1095 days of data are in the order of 0.13 mm/yr for those stations supplying nearly continuous observations. As the adjustment is based on daily free network solutions, the quoted standard deviations may be considered realistic accuracy measures. This is supported by the small differences of 0.2 mm/yr between the uplift rates resulting for two pairs of stations located very close to each other. An effect which has not been modeled in this analysis is hydrological loading (van Dam et al. 2001). This seasonal effect with amplitudes probably well below one centimetre should not affect the vertical velocity estimates, but it could partly be absorbed by the annual signals. It appears that the identification and proper modelling of short period local height biases caused by snow accumulation on the GPS antenna or its radome is an important issue. If not accounted for, this phenomenon will affect the estimates of site dependent pressure loading coefficients.

Acknowledgement

The GPS observations were retrieved from global IGS data centers or the regional data center at the Bundesamt für Kartographie und Geodäsie, Frankfurt, respectively. IGS products were available at the IGS Central Bureau. Dr. H.-G. Scherneck provided the local amplitudes and phases for modelling the ocean loading effects.

References

- Altamimi, Z., Sillard, P., Boucher, C.: A new release of the International Terrestrial Reference Frame for earth science applications. *J. Geophys. Res.* 107, (B10), ETG 2-1 – ETG 2-19, 2002.
- Blewitt, G., Lavallée, D.: Bias in geodetic site velocity due to annual signals: Theory and assessment. *IAG Symposia* 125, 499–500, Springer Berlin Heidelberg New York, 2002a.
- Blewitt, G., Lavallée, D.: Effect of annual signals on geodetic velocity. *J. Geophys. Res.* 107 (B7), ETG 9-1 – ETG 9-11, 2002b.
- van Dam, T., Wahr, J., Milly, P. C. D., Smakin, A. B., Blewitt, G., Lavallée, D., Larson, K. M.: Crustal displacement due to continental water loading. *Geophys. Res. Lett.* 28, 651–654, 2001.
- Huber, S., Kaniuth, K.: On the weighting of GPS phase observations in the EUREF network processing. Presented at the EUREF Symposium 2003, to be published in *Mitt. des Bundesamtes für Kartographie und Geodäsie*, 2004.
- Hugentobler, U., Schaer, S., Fridez, P. (Eds.): *Bernese GPS software version 4.2*. Astron. Inst., University of Berne, 2001.
- Jaldehyag, R. T. K., Johansson, J. M., Davis, J. L., Elósegui, P.: Geodesy using the Swedish permanent GPS network: Effects of snow accumulation on estimates of site position. *Geophys. Res. Lett.* 23, 1601–1604, 1996.
- Johansson, J. M., Davis, J. L., Scherneck, H. G., Milne, G. A., Vermeer, M., Mitrovica, J. X., Bennet, R. A., Ekman, M., Elgered, G., Elósegui, P., Koivula, H., Poutanen, M., Rönnäng, B. O., Shapiro, I. I.: Continuous GPS measurements of postglacial adjustment in Fennoscandia, 1. Geodetic results. *J. Geophys. Res.* 107 (B8), ETG 3-1 – ETG 3-27, 2002.
- Kaniuth, K., Huber, S.: An assessment of radome effects on height estimates in the EUREF network. *Mitt. des Bundesamtes für Kartographie und Geodäsie* 29, 97–102, 2003a.
- Kaniuth, K., Huber, S.: Nachweis von Höhenänderungen aufgrund atmosphärischer Druckvariationen aus GPS-Messungen. *zfv* 128, 278–283, 2003b.
- Lefèvre, F., Lyard, F., Le Provost, C.: FES98: A new global tide finite element solution independent of altimetry. *Geophys. Res. Lett.* 27, 2717–2720, 2000.
- Lemoine, F. G., Kenyon, S. C., Factor, J. K., Trimmer, R. G., Pavlis, N. K., Chinn, D. S., Cox, C. M., Klosko, S. M., Luthcke, S. B., Torrence, M. H., Wang, Y. M., Williamson, R. G., Pavlis, E. C., Rapp, R. H., Olson, T. R.: The development of the joint NASA GSFC and the National Imagery and Mapping Agency (NIMA) geopotential model EGM96. *NASA/TP-1998-206861*, 1998.
- Mäkinen, J., Koivula, H., Poutanen, M., Saaranen, V.: Vertical velocities in Finland from permanent GPS networks and from repeated precise levelling. *J. Geodynamics* 35, 443–456, 2003.
- Niell, A. E.: Global mapping functions for the atmospheric delay at radio wavelengths. *J. Geophys. Res.* 101 (B2), 3227–3246, 1996.
- Scherneck, H.-G., Johansson, J. M., Koivula, H., van Dam, T., Davis, J. L.: Vertical crustal motion observed in the BIFROST project. *J. Geodynamics* 35, 425–441, 2003.

Authors' address

Klaus Kaniuth
Sandra Vetter (geb. Huber)
Deutsches Geodätisches Forschungsinstitut (DGFI)
Marshallplatz 8, D-80539 München, Germany
mailer@dgfi.badw.de